Supplementary to:

Divergent bleaching and recovery trajectories in reef-building corals following a decade of successive marine heatwaves

Kristen T. Brown, Elizabeth A. Lenz, Benjamin H. Glass, Elisa Kruse, Rayna McClintock, Crawford Drury, Craig E. Nelson, Hollie M. Putnam, and Katie L. Barott*

*Correspondence to: kbarott@sas.upenn.edu

Methods

Study site and temperature data

This study was conducted at Patch Reef 13 (PR13) in the southern end of Kāneʻohe Bay, Oʻahu, Hawaiʻi (21.4509, -157.7954). Hourly seawater temperatures were recorded continuously from January 2014 to April 2023 from temperature sensors within the reef at PR13 (1–2.7 m depth) as well as at two adjacent locations within 0.5 km: (1) PR12 (21.45096,-157.7972; 1.5 m depth) and (2) the National Oceanic and Atmospheric Administration (NOAA) Pacific Marine Environmental Laboratory (PMEL) 'CRIMP2' buoy (21.458, -157.798; 0.7 m depth) (Fig. 1, Fig. S1, Table S1). Mean daily (24 hours) seawater temperatures were calculated and averaged when data sources were overlapping, and used to determine cumulative heat stress (degree heating weeks; DHW) at PR13 following the equations in (1) (Fig. 1, Fig. S2, Table S2). The climatic maximum monthly mean (MMM) for Kāneʻohe Bay was determined from seawater temperature data from two monitoring stations on the reefs surrounding the island of Moku o Loʻe (PR1), located approximately 2 km from the study site in the southern region of Kāneʻohe Bay: 1) NOAA's MOKH1 Station[1] (21.433, -157.790; 1.7 m depth) and 2) the HIMB Point Lab Weather Station[2] (21.433, -157.7863; 1 m depth; (2)). Data from 1992–2002 (excluding the 1996 marine heatwave) provided the closest available 10-year data to the time period used by NOAA for determining climatology MMM (1985–1990, 1993), resulting in a climatology MMM for Kāneʻohe Bay of 27.3°C. This MMM was used here to calculate DHW from 2014–2023. Cumulative heat stress at PR13 was compared to PR1 (21.4438, -157.7883; 1 m depth) (Table S1, Fig. S1). DHWs were also calculated from the temperature data recorded at both PR1 and PR13 using the MMM of 27.0°C (Main Hawaiian Island MMM as determined by NOAA and Kāneʻohe Bay climatology MMM from the 1960s (3)), and other recent MMM values used for Kāneʻohe Bay in the literature: 27.7°C (4, 5) and 28.0°C (5, 6) (Fig. S2).

Coral colony selection

All colonies followed in this study were first categorized as bleaching-susceptible (severely bleached) or bleaching-resistant (fully pigmented) based on their bleaching phenotype during the peak of the 2015 heatwave and coral bleaching event (7). For this study, ten pairs of adjacent conspecific colonies of *M. capitata* and *P. compressa* with contrasting bleaching susceptibilities (N=10 colonies per species per phenotype) were selected. Adjacent pairs of

[1] https://www.ndbc.noaa.gov/station_page.php?station=mokh1
[2] http://www.pacioos.hawaii.edu/weather/obs-mokuoloe/#about

bleaching-resistant and bleaching-susceptible colonies of the same species were selected in order to minimize the influence of microenvironment on the bleaching response. Individual colonies were monitored for bleaching (color/pigmentation) and partial mortality from 2015–2017 (7) and 2019–2023 (this study), and sampled for physiological assessments from 2019–2023 (Tables S3 and S4). An additional pair of *M. capitata* and two pairs of *P. compressa* were added to the time series in 2022 to supplement our observations after three pairs could no longer be located; all of these colonies had been assessed for bleaching, mortality and recovery from 2015–2017.

Nearly all of the *M. capitata* colonies used in this study (20 of the 22 colonies) were identified as unique genotypes in an earlier study (8). In general, clonality in *M. capitata* in Kāne‘ohe Bay is very low (9), with a bay-wide genet-ramen ratio of 0.917. Caruso et al (2022) included two sites at the same reef investigated in this study (Patch Reef 13), identifying a genet-ramen (G:R) ratio of 0.95 (i.e., 21 genotypes in 22 colonies sampled). For *P. compressa*, the bay-wide genet-ramen ratio is approximately 0.875, but clonality is rare in low wave energy (inner bay) environments (10). Similarly, *P. compressa* from sheltered South Bay sites have a genet-ramen ratio of 0.96 (11). The likelihood of there being more than three clones in *P. compressa* is very low (0.92 [average of two papers G:R] * 24 colonies = 22 genotypes), especially considering the physiological variation observed. Overall, these studies indicate infrequent asexual reproduction at the study site for either species.

Coral bleaching and partial mortality assessments

Colony-level bleaching severity was determined from photographs of each colony following the methodology of (6), in which colonies were scored as: (1) no signs of paling (0%), (2) mild paling (>20%), (3) moderate paling (20–50%), (4) mostly bleached (50–80%), and (5) fully bleached (80–100%). Cumulative colony-level partial mortality was also determined from these same photographs as described in (7), where the partial mortality of each colony was visually estimated to the nearest 10%. Observations occurred during peak and off-peak seasonal temperatures in most years. Benthic community composition was determined at the same time as colony-level observations following the same methods as in (6, 7). Specifically, benthic photoquadrats (0.33 m^2), were imaged at 2 m intervals along a 40 m transect tape laid parallel to the reef crest at 1 m and 3 m depths (n = 1–2 per depth) at PR13. Benthic community composition was determined from each image via CoralNet using 50 randomly allocated points per photograph (12). Bleaching severity of each coral point was scored as: (1) pigmented (no signs of bleaching), (2) pale (moderately bleached), or (3) severely bleached (white). Reef-wide bleaching prevalence for each species was determined as the proportion of observations of that species showing signs of moderate or severe bleaching (i.e. bleaching score of 2 or 3).

Physiological analyses

A total of 276 fragments were collected from colonies of bleaching-resistant and bleaching-susceptible *M. capitata* and *P. compressa* (n= 7–10 pairs per phenotype per species) across eight timepoints from October 2019 to September 2022, incorporating the peak of the 2019 heatwave and three years (35 months) of recovery during non-heatwave years (Fig. S1). Fragments (4–5 cm in length) were collected by hand using bone cutters, transported to the

Hawai'i Institute of Marine Biology (HIMB) in ambient seawater and held in flow-through seawater aquaria for 24–72 hours until measurements of coral performance. For four timepoints (October 2019, October 2021, March 2022, and September 2022), metabolic rates were assessed via changes in oxygen evolution using oxygen optodes (PSt7, PreSens) connected to an optical analyser (OXY-10, PreSens) (6). Oxygen optodes were calibrated on each day with a 0% oxygen solution (0.01 g ml^{-1} $NaSO_3$) and 100% air saturated seawater. Coral fragments were analyzed between 08:00 and 17:00 within 250 ml clear acrylic chambers on top of a magnetic stirrer to allow for continuous mixing. Seawater temperatures were replicated to those experienced on the reef by using ambient seawater and a water jacket to maintain temperatures within the incubation chambers. Temperature and dissolved oxygen concentrations were recorded every 3 seconds at increasing increments of light over a total of 45–50 minutes to determine maximum net photosynthesis (Pmax). Light levels ranged from 112–726 µmol m^{-2} sec^{-1} in October 2019 (6) (step size ~100 µmol m^{-2} sec^{-1}; ~10 minutes $step^{-1}$), and from 387–1800 µmol m^{-2} sec^{-1} in 2020–2021 (step size ~300 µmol m^{-2} sec^{-1}; ~10 minutes $step^{-1}$). After measurements were completed at the maximum light levels, the lights were turned off (0 µmol m^{-2} sec^{-1}) to measure light-enhanced dark respiration (LEDR) as defined by (13). Photosynthesis-irradiance curves were fitted using the Platt model to extract Pmax and LEDR (6, 14). Upon completion of these *in vivo* analyses, coral fragments were flash frozen in liquid nitrogen and stored at −80°C until further processing.

Coral tissues containing symbionts were removed from skeletons with a waterpik using 50 mL of 0.1 M phosphate buffered saline (PBS) solution. The resulting holobiont homogenate was centrifuged at 4°C for 5 minutes at 2500 x g to separate the coral host fraction (supernatant) from the intracellular endosymbiont cells (family Symbiodiniaceae; pellet). Symbiodiniaceae were resuspended in PBS and cell abundances were quantified using a Millipore Guava flow-cytometer (Guava easyCyte 5HT) following the methodology of (6). Symbiodiniaceae cells were excited with a blue laser (488 nm) and identified by analyzing forward scatter and red autofluorescence in GuavaSoft 3.4 with the same gating for all samples. Symbiont densities were standardized to skeletal surface area (cm^2), which was determined using the wax-dipping technique (15, 16). Endosymbiont photopigments were extracted in 100% acetone for 24 hours and the concentration of chlorophyll-*a* was determined via absorbance at 630, 663, and 750 nm using the equation in (17) and subtracting the absorbance at 750 nm from both A663 and A630:

$$Chlorophyll\ a\ = (11.43\ \times (A663\ -\ A750))\ -\ (0.64\ \times (A630\ -\ A750))$$

Photopigment concentrations were standardized to both skeletal surface area and symbiont densities. Endosymbiont community composition (proportion *Durusdinium* vs. *Cladocopium*) of *M. capitata* colonies was determined by Dilworth et al. 2021 from samples collected in July 2019 using quantitative PCR.

Host tissue biomass was determined as ash-free dry weight (AFDW) from the coral fraction (i.e. symbionts removed as described above). First, 1 mL of the coral fraction was dried at 60°C for 24 hours until a constant weight was achieved. After the dry weight was recorded, the samples were then burned in a muffle furnace at 450°C for 6 hours. The samples were allowed to cool in

the furnace before being weighed and the weight of the resulting ash was recorded. The difference between the ash weight and the dry weight was calculated to determine the AFDW of each sample. Host soluble protein content of each sample was determined via the Bradford method. Specifically, 10 µL of the coral fraction was pipetted into each of three wells of a 96-well plate (technical replicates), followed by the addition of 300 µL of Coomassie Plus Bradford reagent (Thermo Fisher Scientific) to each well. The plate was incubated for 10 minutes at room temperature followed by the collection of an absorbance reading at 595 nm on a spectrophotometer (BioTek PowerWave XS2). Each plate contained a set of internal standards with known concentrations of bovine serum albumin (0–2000 µg mL^{-1}), which were used to generate a second-degree polynomial standard curve relating absorbance (x) to protein concentration (y). The standard curve equation was used to calculate the protein concentrations of the samples. The concentration of lipids in each sample was determined via a modified method of (18). First, ~45 mL of the coral fraction was lyophilized to produce dry tissue. A subsample of the lyophilized tissue was weighed (~90 mg), and 2 mL of chloroform-methanol (2:1) was added. The sample was then mixed using a homogenizer at 15000 rpm for 5 seconds, and an additional 2 mL of chloroform-methanol was used to rinse the homogenizer into the sample, and the tubes were then vigorously vortexed before being placed at 4°C for 2 hours in the dark. After incubation, tubes were again vortexed and the chilled homogenates were then passed through 0.22 µm syringe filters into new pre-weighed tubes. An additional 1 mL of chloroform-methanol was passed through the filters into each tube to ensure the full passage of sample material. Next, 1 mL of 0.1 M KCl was added to the samples, which were then vortexed and placed at 4°C for at least 1 hour in the dark until two phases formed. The aqueous (top) phase was discarded, and 5 mL of 50% methanol was added to the organic (bottom) phase. The samples were then placed at 4°C for 1 hour in the dark, followed by removal of the aqueous (top) phase. Washes with 50% methanol were repeated twice more, and the remaining organic phases were dried under a fume hood until the solvent had completely evaporated, at which point the lipid pellet was weighed. Coral host biomass, protein and lipid content were standardized to skeletal surface area.

The total antioxidant capacity of the coral homogenate was assessed using a kit from Cell Biolabs (STA-360) according to the manufacturer's instructions. First, 20 µL of the coral fraction was transferred to each of two wells of a 96-well plate (technical replicates), followed by the addition of 1x reaction buffer (20 µL) from the kit. An initial absorbance reading was collected with a spectrophotometer at 490 nm. Next, 50 µL of 1x copper ion reagent were added to each well, followed by incubation for 5 minutes with gentle shaking. Following shaking, 50 µL of 1x stop solution was added to each well, and a second absorbance reading was collected at 490 nm. Each plate contained a set of standards with known concentrations (0–0.1 mM) of uric acid. For analysis, the initial absorbance readings were subtracted from the final absorbance readings for each standard well, and the resulting values were used to generate a linear standard curve relating the absorbance (x) to the concentration of uric acid (y). The standard curve equation was used with the average change in absorbance across the two technical replicates for each sample to first determine the concentration of uric acid equivalents in the samples, which was then converted to a concentration of copper reducing equivalents (CRE) using the equivalence of 1 mM of uric acid to 2189 µM CREs. Finally, the CRE values were

normalized to the amount of protein in each well, for a final value of TAC expressed as μM CRE mg protein^{-1}.

To assess the melanin content of the coral homogenate, a protocol was adapted from (4). First, 1.5 mL tubes were filled with approximately 20 mg of the dry coral fraction and the weight recorded. Next, 300 μL of 10 M NaOH was added to each tube, followed by vortexing for 20 seconds. Samples were left overnight at room temperature in the dark, then vortexed again for 10 seconds before being centrifuged at 7000 x g for 5 minutes. Following centrifugation, 100 μL of supernatant was transferred to each of two wells of a 96-well plate (technical replicates), which was then read for absorbance on a spectrophotometer at 490 nm. Each plate contained a set of internal standards with known concentrations (0–0.01 mg mL^{-1}) of synthetic melanin (M8631, Sigma Aldrich) in 10 M NaOH, which were used to generate a linear standard curve relating absorbance (x) to melanin concentration (y). The standard curve equation was then used to calculate the concentration of melanin in each sample, which was standardized to the original weight of the dry coral host tissue used in the assay.

A protocol was adapted from (4, 19, 20) to assess the content of prophenoloxidase (PPO) in each coral sample. First, 150 μL of the coral fraction was transferred to each of two wells of a 96-well plate (technical replicates). Next, 23 μL of 0.2 mg mL^{-1} trypsin was added to each well, and the plate was incubated for 5 minutes at room temperature with shaking. Following incubation, 60 μL of 10 mM L-1,3- dihydroxyphenylalanine (L-DOPA) was added to all wells, and the plate was again incubated at room temperature for 5 minutes with shaking. Next, the plate was read for absorbance on a spectrophotometer at 490 nm every minute for 15 minutes. The absorbance of each well at the start of the 15 minutes was subtracted from the absorbance of the same well at the end, and values were divided by 15 to determine the change in absorbance per minute, which were then averaged over the two technical replicates. Finally, these values were standardized to the amount of protein in each well for a final quantification of PPO activity expressed as the change in absorbance minute^{-1} mg protein^{-1}.

Wax-dipping was used to determine calcium carbonate ($CaCO_3$) bulk density, where the skeleton was cleaned, dried to a constant mass and weighed, sealed with a coat of wax, dry weighed with the wax and then buoyant weighed in DI water at 20°C (21, 22). The difference between dry weight (with wax) and buoyant weight (divided by the density of the DI water medium of 1 mg cm^{-3}) was calculated to determine the total volume enclosed. The dry skeletal mass (wax free) was then divided by the total volume enclosed to yield bulk density (g cm^{-3}).

Acute heat stress experiment

Ten individual colonies of each phenotype per species were sampled on September 1, 2022. Four fragments were collected from each individual colony (i.e., genetic clones) by hand using bone cutters, totalling 160 fragments. Following collection, corals were transported to the Hawai‘i Institute of Marine Biology (HIMB) and placed in outdoor, flow-through seawater tanks under ambient temperatures (mean ± SD; 28.2 ± 0.1°C, n=2 tanks) until experimentation. Coral thermal tolerance experiments were initiated 72 hours after collection. The experimental heat stress assay followed the standardized temperature profile used to measure heat tolerance in

corals (e.g., MMM, MMM+3°C, MMM+6°C, and MMM+9°C) (23). The experiment began on September 4 2022 at 13:00 with a 3-hour ramp to respective treatment temperatures (27.5°C, 30.5°C, 33.5°C, 36.5°C), a 3-hour hold, and a 1-hour ramp down to MMM temperature (27.5°C). A fragment from each coral colony was suspended using fishing line and randomly placed into each treatment, so that all genotypes across species were present in each treatment. Temperatures were controlled using a custom computer controlled system (Raspberry Pi). Temperatures were constantly monitored and manipulated by responding to probe measurements in real time, and recorded using cross-calibrated temperature loggers (accuracy: ± 0.47°C at 25°C; resolution: ± 0.10°C at 25°C HOBO UA-001-64, Onset Computer Corporation). Experiments were performed outdoors under natural photosynthetically active radiation (PAR), which ranged between 515–580 µmol m^{-2} sec^{-1} at midday (~12:00; Licor cosine sensor). At the end of the ramp and 1 h after sunset (~19:30), corals were assessed for dark-adapted photochemical yield (F_v/F_m) using a Diving-PAM (Walz GmbH) 5-mm diameter fiber-optic probe at a standardized distance (5 mm) above the coral tissue after F_0 stabilized. Three random spots (2–3 cm apart across the front and back of the nubbin) were measured on each fragment to obtain average measures of F_v/F_m. All readings with F_0 values that were less than 110 were removed to avoid any false detections (24). The following morning at 07:00 corals were photographed with a color standard (WDKK Waterproof Color Chart, DGK Color Tools) to assess coral color, a proxy for bleaching severity. Bleaching severity was determined visually (e.g., 0, 20, 40, 60, 80, 100% white) (25) using the six gray standards as a reference (e.g., black= 0% bleached, white = 100% bleached) from two photographs (front and back of the fragment) to obtain an average color score (Fig. S4).

Statistical analyses

Graphical representations were produced using the package *ggplot2 (26)*. For colony-level bleaching severity, the interactive effects of phenotype (bleaching-susceptible, bleaching-resistant), coral species (*M. capitata*, *P. compressa*), season (summer: May, June, July, August, September, October; winter: November, December, January, February, March, April), and year (May 2015– April 2016, 2016–2017, 2017, 2019–2020, 2020–2021,2021–2022, 2022) were explored using a linear model. To assess differences in physiological parameters (total biomass, host soluble protein, lipids, $CaCO_3$ density, TAC, melanin content, PPO activity, CS, endosymbiont density, chlorophyll-*a* content) between phenotype, coral species and months post-heat stress (0, 10, 13, 17, 20, 24, 29, 35), linear mixed effects (lme) models were used, with genet (i.e., colony ID) included as a random effect. The significance of fixed effects and their interactions was determined using an analysis of variance with a type III error structure using the Anova function in the *car* package (27). Significant interactive effects were followed by pairwise comparison of estimate marginal means using the *emmeans* package with Tukey HSD adjusted p values (28). Data were tested for homogeneity of variance and normality of distribution through graphical analyses of residual plots for all models.

Differences in temperature profiles of the experimental stress assays (four levels: ambient, ambient+3°C, ambient+6°C, ambient+9°C) were explored using a linear model. To determine how heat tolerance differed amongst coral species and phenotype, three-parameter log-logistic dose-response curves were fit to the average dark-adapted photochemical yield (F_v/F_m) across

temperature treatments using the function dose-response model, drm, in the package *drc* (29). From these dose-response curves, the effective temperature to induce a 50% loss in F_v/F_m (effective dose 50; ED50) was calculated as the F_v/F_m or color score from the model fit that is 50% of the initial value (25).

Differences in coral multivariate phenotypes were analyzed separately for each coral species using permutational multivariate analysis of variance (PERMANOVA) and principal components analysis (PCA), with the fixed effects phenotype and months post-heat stress using the adonis and rda functions in the *vegan* package, respectively (30). Significant effects were followed by pairwise comparisons using the pairwiseAdonis2 function in the *pairwiseAdonis* package (31). Resemblance matrices were obtained using Bray-Curtis dissimilarity and 9999 permutations.

Results

Metabolic rates

Maximum net photosynthesis (P_{max}) ($\chi^2 = 11.8$, $p = 0.008$) and light-enhanced dark respiration (LEDR) ($\chi^2 = 11.8$, $p = 0.008$) were significantly influenced by the interaction between coral species and time. Pairwise comparisons revealed that across all timepoints, P_{max} and LEDR were greater in *P. compressa* than *M. capitata* ($p < 0.001$), and no significant differences were found between timepoints for either species ($p > 0.16$) (Fig. 3, Fig. S4). Photosynthesis to respiration (P:R) rates were significantly influenced by phenotype ($\chi^2 = 4.1$, $p = 0.04$), where bleaching-resistant corals trended towards higher P:R rates than bleaching-susceptible conspecifics (Fig. 3, Fig. S4).

Immunity and antioxidant metrics

Total antioxidant capacity (TAC) was significantly influenced by the interaction between coral species and time ($\chi^2 = 24.2$, $p = 0.001$). For *M. capitata*, TAC was highest in October 2021 and significantly greater than the same time during the previous year (November 2020), as well as in comparison to the marine heatwave (October 2019) ($p < 0.003$) (Fig. 3g, Fig. S4). Similarly for *P. compressa*, TAC was significantly greater in November 2020 and October 2021 when compared to the 2019 marine heatwave ($p < 0.05$) (Fig. 3g, Fig. S4).

Melanin content was significantly influenced by the interaction between coral species and time ($\chi^2 = 17.1$, $p = 0.009$). Melanin concentrations were not measured during the 2019 marine heatwave. Across the time series, *P. compressa* had higher melanin concentrations than *M. capitata* ($p < 0.002$) (Fig. 3h, Fig. S4). For *M. capitata*, melanin concentrations did not differ between time points ($p > 0.27$), whereas for *P. compressa*, seasonal patterns were observed with concentrations generally greatest between March–June, yet also elevated in October 2021 (Fig. 3h).

Prophenoloxidase (PPO) activity was significantly influenced by the three-way interaction between coral species, phenotype and time ($\chi^2 = 18.2$, $p = 0.006$). Pairwise comparisons revealed that bleaching-susceptible *P. compressa* had lower PPO activity than bleaching-resistant corals 13 months post-heat stress and bleaching-susceptible *M. capitata* had lower PPO activity than bleaching-resistant conspecifics 17 months post-heat stress (Fig.

3i, Fig. S4). For several time points (13, 24, and 29 months post-heat stress), *P. compressa* had greater PPO activity than *M. capitata*, particularly bleaching-resistant comparisons ($p < 0.04$). PPO activity was significantly lower in August–September (10 months and 35 months post-heat stress) than all other time points regardless of coral species or phenotype ($p < 0.05$) (Fig. 3i, Fig. S4).

Short-term heat stress experiment

Color score, as a proxy for bleaching severity, was significantly influenced by the interaction between species and phenotype ($X^2 = 4.1$, $p = 0.04$) as well as individual effect of temperature ($X^2 = 134.1$, $p < 0.0001$). There were no significant differences in F_v/F_m between *M. capitata* and *P. compressa* at ambient ($p = 0.09$), +3°C ($p = 0.06$), or +6°C ($p = 0.08$), yet in the hottest treatment (+9°C), *P. compressa* F_v/F_m was significantly greater than *M. capitata* ($p < 0.0001$) (Fig. 5). Pairwise comparison revealed no differences in bleaching severity between phenotypes of *P. compressa* ($p = 0.85$), yet for *M. capitata*, susceptible corals were significantly paler than resistant conspecific corals ($p < 0.0001$) (Fig. S6b). Regardless of species, bleaching severity increased across all treatments ($p <0.0001$), with the exception of ambient and +3°C ($p = 0.65$). Interestingly, heat tolerance (ED50) determined through color score was between 1.9 – 2.8°C lower than that determined via photochemical yield and there was only 0.4°C difference in the color score ED50 between the least and most heat tolerant species.

Supplementary Figures and Tables

Table S1. Temperature metadata. Abbreviations: NOAA = National Oceanic and Atmospheric Administration, PMEL = Pacific Marine and Environmental Laboratory

Contributor	Reef	Coordinates	Date range	Sensor type	Sampling interval	Depth (m)
NOAA - PMEL	CRIMP2	21.458, -157.798	2013-11-28 to 2020-03-30*	SBE 37 SMP[1]	3 hours	0.7
HIMB weather station	Reef 1	21.433, -157.7863	2014-01-01 to 2022-11-22*	BetaTherm 100K6A1IA Thermistor[2]	1 hour	1.0
Division of Aquatic Resources (DAR)	Reef 12	21.45096, -157.79723	2015-06-19 to 2016-01-21	Onset Pro v2[3]	15 minutes	DH 1.5
		21.45090, -157.79729				
Gates Lab (Katie Barott)	Reef 13	21.4516, -157.7966	2016-07-06 to 2017-04-18	SBE Sea-pHOx[1]	15 minutes	2.0
Coral Reef Resilience Lab (Carlo Caruso, Crawford Drury, Mariana Rocha de Souza)	Reef 13	21.4518, -157.7956	2019-09-27 to 2021-08-26	Onset Pro v2[3]	10 minutes	1.2
		21.4509, -157.7954				1.7
		21.4518, -157.7956	2022-02-26 to 2022-11-28			1.2
		21.4509, -157.7954				1.7
Barott Lab (Kristen Brown and Katie Barott)	Reef 13	21.4516, -157.7965	2022-09-02 to 2023-04-13	Onset Pro V2[3]	30 minutes	1.0
		21.4507, -157.7962				1.0
		21.4517, -157.7967				2.5

*Incomplete record.

[1]Accuracy: ±0.002°C; resolution: 0.0001°C at 25°C

[2]Tolerance: ±0.2°C; Steinhart-Hart equation error: ≤ ±0.01°C at 25°C

[3]Accuracy: ±0.21°C; resolution: 0.02°C at 25°C

Table S2. Comparison of maximum cumulative degree heating weeks from 2014–2022. Light gray shading indicates years with recognized marine heatwaves.

Maximum cumulative degree heating weeks					
Location	Kāneʻohe Bay^				Main Hawaiian Islands*
Temperature dataset	Reef 13	Reef 1 (Moku o Loʻe)	Reef 13	Reef 1 (Moku o Loʻe)	NOAA (SST)
Year	24 hour mean; Local MMM (27.3°C)		24 hour mean; Regional MMM (27.0°C)		Nighttime mean; Regional MMM (27.0°C)
2014	7.3	5.2	10.2	9.0	4.5
2015	8.8	7.2	14.6	11.2	12.5
2016	0	0	0.2	0.3	0
2017	0.6	0	3.2	2.0	1.3
2018	0.8	0.6	2.0	1.5	0.15
2019	5.1	10.2	10.2	15.3	13.6
2020	0.1	0.2	3.1	1.0	0.5
2021	0	0.2	0.7	0.7	0
2022	0.2	0.6	2.9	2.1	0

^Kāneʻohe Bay data are from *in situ* temperature loggers (depth 0.7 – 2.7 m; as described in Table S1).

*Main Hawaiian Islands data are from NOAA satellite-derived sea surface temperature (SST).

Table S3. Sample collection record for *Montipora capitata* colonies from 2019–2023. All colonies were designated bleaching-susceptible or bleaching-resistant based on their bleaching phenotype during the peak of the 2015 heatwave and coral bleaching event (7). Each colony was imaged for color score and a fragment was collected for physiological analysis at each time point, except where indicated. Y, yes sampled; N, not sampled.

		Sampling date																	
		2019						2020					2021				2022		2023
Susceptible coral ID	**Resistant coral ID**	Jun 28*	Jul 19*	Sep 16*#	Oct 2#	Oct 16*#	Oct 30*#	Jan 24*	Aug 27	Oct 8*	Nov 5	Dec 10*	Mar 23	Jun 25	Sep 13*	Oct 8	Mar 9	Sep 1	Apr 13*
3	4	Y	Y	Y	Y	Y	Y	Y	Y	Y	Y	Y	Y	Y	Y	Y	Y	Y	Y
11	12	N	Y	Y	Y	Y	Y	Y	Y	Y	Y	Y	Y	Y	Y	Y	Y	Y	Y
19	20	Y	Y	Y	Y	Y	Y	Y	Y	Y	Y	Y	Y	Y	Y	Y	Y	Y	Y
201	202	Y	Y	Y	Y	Y	Y	Y	Y	Y	Y	Y	Y	Y	Y	Y	Y	Y	Y
203	204	Y	Y	Y	Y	Y	Y	Y	Y	Y	Y	Y	Y	Y	Y	Y	Y	Y	Y
209	210	N	Y	Y	Y	Y	Y	Y	Y	Y	Y	Y	Y	N	Y	Y	Y	Y	Y
211	212	Y	Y	Y	Y	Y	Y	Y	Y	Y	Y	Y	Y	Y	Y	Y	Y	Y	Y
213^	214^	N	N	N	N	N	N	N	N	N	N	N	N	N	N	N	N	Y	Y
217	218	N	Y	Y	Y	Y	Y	Y	Y	Y	Y	Y	Y	Y	Y	N	N	N	Y
219	220	N	Y	Y	Y	Y	Y	Y	Y	Y	Y	Y	Y	Y	Y	Y	Y	Y	Y
221	222	Y	Y	Y	Y	Y	Y	Y	Y	Y	Y	Y	Y	N	Y	Y	Y	Y	Y
Total colony pairs (N)		**6**	**10**	**10**	**10**	**10**	**10**	**10**	**10**	**10**	**10**	**10**	**10**	**8**	**10**	**9**	**9**	**10**	**11**

*Color scores only

^Added in 2022 to supplement lost pairs

#Physiology data from (6)

Table S4. Sample collection record for *Porites compressa* colonies from 2019–2023. All colonies were designated as bleaching-susceptible or bleaching-resistant based on their phenotype during the peak of the 2015 heatwave and coral bleaching event (7). Each colony was imaged for color score and a fragment was collected for physiological analysis at each time point, except where indicated. Y, yes sampled; N, not sampled.

		Sampling date																	
		2019						2020					2021				2022		2023
Susceptible coral ID	**Resistant coral ID**	Jun 28*	Jul 19*	Sep 16*#	Oct 2#	Oct 16*#	Oct 30*#	Jan 24*	Aug 27	Oct 8*	Nov 5	Dec 10*	Mar 23	Jun 25	Sep 13*	Oct 8	Mar 9	Sep 1	Apr 13*
27	26	Y	Y	Y	Y	Y	Y	Y	Y	Y	Y	Y	Y	Y	Y	Y	Y	Y	Y
35	36	N	Y	Y	Y	Y	Y	Y	N	N	N	N	N	N	N	N	N	N	N
41	42	Y	Y	Y	Y	Y	Y	Y	Y	Y	Y	Y	Y	Y	Y	Y	Y	Y	Y
43	44	Y	Y	Y	Y	Y	Y	Y	Y	Y	Y	Y	Y	Y	Y	Y	Y	Y	Y
45	46	Y	Y	Y	Y	Y	Y	Y	Y	Y	Y	Y	Y	Y	Y	Y	Y	Y	Y
225^	226^	N	N	N	N	N	N	N	N	N	N	N	N	N	N	N	N	Y	Y
229	230	Y	Y	Y	Y	Y	Y	Y	Y	Y	Y	Y	Y	Y	Y	N	N	N	N
235^	236^	N	N	N	N	N	N	N	N	N	N	N	N	N	N	N	N	Y	Y
237	238	Y	Y	Y	Y	Y	Y	Y	Y	Y	Y	Y	Y	Y	Y	Y	Y	Y	Y
239	240	Y	Y	Y	Y	Y	Y	Y	Y	Y	Y	Y	Y	Y	Y	Y	Y	Y	Y
243	244	Y	Y	Y	Y	Y	Y	Y	Y	Y	Y	Y	Y	Y	Y	Y	Y	Y	Y
247	248	Y	Y	Y	Y	Y	Y	Y	Y	Y	Y	Y	Y	Y	Y	Y	Y	Y	Y
Total colony pairs (N)		**9**	**10**	**10**	**10**	**10**	**10**	**10**	**9**	**9**	**9**	**9**	**9**	**9**	**9**	**8**	**8**	**10**	**10**

*Color scores only

^Added in 2022 to supplement lost pairs

#Physiology data from (6)

Table S5. Full statistical results for in situ colony-level bleaching severity. R^2c indicates the conditional R^2 (e.g., assessment of model fit). Bolding indicates significant p values.

Response variable	Fixed effects	R^2c	Sum of squares	Degrees of freedom	F value	p value Pr(>F)
Colony-level bleaching severity	Phenotype	0.63	190.35	1	486.1624	**< 2.2e-16**
	Species		95.47	1	243.883	**< 2.2e-16**
	Season		60	1	153.2798	**< 2.2e-16**
	Time		65.95	6	28.0796	**< 2.2e-16**
	Phenotype:Species		74	1	189.0204	**< 2.2e-16**
	Phenotype:Season		35.24	1	90.0245	**< 2.2e-16**
	Species:Season		11.72	1	29.9432	**5.75E-08**
	Phenotype:Time		60.49	6	25.7517	**< 2.2e-16**
	Species:Time		11.11	6	4.7288	**9.39E-05**
	Season:Time		19.35	4	12.3558	**8.66E-10**
	Phenotype:Species:season		2.37	1	6.0537	**0.01406**
	Phenotype:Species:Time		2.76	6	1.1768	0.31636
	Phenotype:Season:Time		29.18	4	18.6327	**9.86E-13**
	Species:Season:Time		14.34	4	9.1584	**2.96E-05**
	Phenotype:Species:Season:Time		9.6	4	6.1294	**7.22E-05**
	Residuals		356.24	910		

Table S6. Full statistical results for in situ colony-level partial mortality. R^2c indicates the conditional R^2 (e.g., assessment of model fit). Bolding indicates significant p values.

Response variable	Fixed effects	R^2c	Random effect variance	Chisq	Degrees of freedom	p value (Pr > Chisq)
Colony-level partial mortality	(Intercept)	0.66	15.1	0	1	1
	Phenotype			0.043	1	0.8357
	Species			0	1	1
	Time			175.8747	14	**< 2.2e-16**
	Species:Phenotype			0.6585	1	0.4171
	Phenotype:Time			4.6515	14	0.9901
	Species:Time			86.9189	14	**1.45E-12**
	Species:Phenotype:Time			20.7339	14	0.1086

Table S7. Coral physiology sample sizes by date, species and phenotype from 2019–2023.

Date	Species	Phenotype	Sample size
2019-10-02	*Montipora capitata*	Susceptible	10
		Resistant	10
	Porites compressa	Susceptible	10
		Resistant	10
2020-08-27	*Montipora capitata*	Susceptible	7
		Resistant	9
	Porites compressa	Susceptible	8
		Resistant	10
2020-11-05	*Montipora capitata*	Susceptible	10
		Resistant	10
	Porites compressa	Susceptible	9
		Resistant	9
2021-03-21	*Montipora capitata*	Susceptible	10
		Resistant	10
	Porites compressa	Susceptible	8
		Resistant	10
2021-06-25	*Montipora capitata*	Susceptible	9
		Resistant	10
	Porites compressa	Susceptible	9
		Resistant	9
2021-10-08	*Montipora capitata*	Susceptible	9
		Resistant	9
	Porites compressa	Susceptible	7
		Resistant	7
2022-03-09	*Montipora capitata*	Susceptible	9
		Resistant	9
	Porites compressa	Susceptible	7

		Resistant	7
2022-09-01	*Montipora capitata*	Susceptible	4
		Resistant	7
	Porites compressa	Susceptible	7
		Resistant	5

Table S8. Full statistical results for in situ physiological metrics. R^2c indicates the conditional R^2 (e.g., assessment of model fit). Bolding indicates significant p values.

Response variable	Fixed effects	R^2c	Random effect variance	Chisq	Degrees of freedom	p value (Pr > Chisq)
Host tissue biomass (ash-free dry weight)	(Intercept)	0.70	1.75	13.03	1	**0.000306**
	Species			7.98	1	**0.004719**
	Phenotype			0.05	1	0.826458
	Months			92.54	7	**< 2.2e-16**
	Species:Phenotype			0.81	1	0.367039
	Species:Months			15.93	7	**0.025739**
	Phenotype:Months			2.10	7	0.953898
	Species:Phenotype:Months			13.73	7	0.056181
Host lipids	(Intercept)	0.41	3.66	42.97	1	**5.56E-11**
	Species			1.19	1	0.2752703
	Phenotype			0.43	1	0.5123488
	Months			26.21	6	**0.0002031**
	Species:Phenotype			0.25	1	0.6170538
	Species:Months			25.20	6	**0.0003136**
	Phenotype:Months			5.17	6	0.5219914
	Species:Phenotype:Months			14.85	6	**0.0214855**
Host soluble protein density	(Intercept)	0.62	0.095	28.02	1	**1.20E-07**
	Species			7.15	1	**0.007495**
	Phenotype			0.11	1	0.740747
	Months			46.23	7	**7.89E-08**
	Species:Phenotype			0.12	1	0.731906
	Species:Months			20.53	7	**0.004532**
	Phenotype:Months			6.38	7	0.495677
	Species:Phenotype:Months			8.27	7	0.309023
Calcium carbonate (CaCO3) density	(Intercept)	0.66	0.20	354.07	1	**< 2.2e-16**
	Species			0.06	1	0.81041
	Phenotype			0.34	1	0.56225
	Months			113.09	7	**< 2.2e-16**
	Species:Phenotype			0.01	1	0.93113
	Species:Months			31.56	7	**4.90E-05**
	Phenotype:Months			14.16	7	**0.04849**

	Species:Phenotype:Months			14.12	7	**0.04909**
Symbiont density	(Intercept)	0.475	0.98	1.34	1	0.24779
	Species			2.06	1	0.15111
	Phenotype			1.15	1	0.28424
	Months			14.91	7	**0.03713**
	Species:Phenotype			0.79	1	0.37539
	Species:Months			16.39	7	**0.02179**
	Phenotype:Months			1.29	7	0.98866
	Species:Phenotype:Months			3.89	7	0.79215
Chlorophyll *a*	(Intercept)	0.71	5.5	5.86	1	**0.0154795**
	Species			46.80	1	**7.87E-12**
	Phenotype			0.96	1	0.3265554
	Months			24.59	7	**0.0008983**
	Species:Phenotype			1.50	1	0.2213852
	Species:Months			12.59	7	0.0828781
	Phenotype:Months			2.25	7	0.944776
	Species:Phenotype:Months			14.96	7	**0.0364776**
Maximum net photosynthesis (Pmax)	(Intercept)	0.59	0.66	78.06	1	**< 2.2e-16**
	Species			4.74	1	**0.029549**
	Phenotype			0.95	1	0.330127
	Months			2.99	3	0.393897
	Species:Phenotype			1.40	1	0.237319
	Species:Months			11.82	3	**0.008044**
	Phenotype:Months			0.53	3	0.912933
	Species:Phenotype:Months			5.93	3	0.114962
Light-enhanced dark respiration (LEDR)	(Intercept)	0.55	0.23	30.51	1	**3.32E-08**
	Species			3.35	1	0.06734
	Phenotype			2.43	1	0.1189
	Months			1.38	3	0.71007
	Species:Phenotype			0.69	1	0.4077
	Species:Months			8.04	3	**0.04523**
	Phenotype:Months			2.80	3	0.42326
	Species:Phenotype:Months			5.43	3	0.14291
Photosynthesis:Respiration (P:R)	(Intercept)	0.29	1.21	143.50	1	**< 2e-16**
	Species			0.44	1	0.50651

	Phenotype			4.14	1	**0.04184**
	Months			1.02	3	0.79632
	Species:Phenotype			0.58	1	0.44675
	Species:Months			2.53	3	0.47024
	Phenotype:Months			5.68	3	0.12812
	Species:Phenotype:Months			1.27	3	0.73596
Total antioxidant capacity (TAC)	(Intercept)	0.20	54412	0.01	1	0.919
	Species			0.10	1	0.7553
	Phenotype			0.00	1	0.9716
	Months			29.74	6	**4.41E-05**
	Species:Phenotype			0.00	1	0.9749
	Species:Months			10.35	6	0.1106
	Phenotype:Months			2.24	6	0.896
	Species:Phenotype:Months			1.81	6	0.9361
Melanin content	(Intercept)	0.70	0.0004	18.54	1	**1.67E-05**
	Species			9.02	1	**0.002678**
	Phenotype			0.48	1	0.488592
	Months			5.62	6	0.467357
	Species:Phenotype			0.01	1	0.909084
	Species:Months			17.07	6	**0.009027**
	Phenotype:Months			1.79	6	0.937914
	Species:Phenotype:Months			5.74	6	0.453467
Prophenoloxidase (PPO) activity	(Intercept)	0.62	0.25	2.86	1	0.090928
	Species			0.10	1	0.749573
	Phenotype			0.17	1	0.678897
	Months			44.63	6	**5.55E-08**
	Species:Phenotype			0.06	1	0.798951
	Species:Months			4.77	6	0.574124
	Phenotype:Months			7.46	6	0.280387
	Species:Phenotype:Months			18.22	6	**0.005698**

Table S9. Full statistical results for the in situ multivariate health metric. Bolding indicates significant p values.

Response variable	Fixed effects	Degrees of freedom	Sum of squares	Mean squares	pseudo-F	R2	p value Pr(>F)
Multivariate health metric - *Montipora capitata*	Bleach	1	0.025	0.025	2.027	0.009	0.1154
	Months	7	1.115	0.159	12.813	0.393	**0.0001**
	Bleach:Months	7	0.129	0.018	1.480	0.045	0.0929
	Residuals	126	1.567	0.012		0.552	
	Total	141	2.836			1.000	
Multivariate health metric - *Porites compressa*	Bleach	1	0.025	0.025	0.956	0.006	0.4775
	Months	7	0.746	0.107	4.103	0.187	**0.0001**
	Bleach:Months	7	0.153	0.022	0.840	0.038	0.7078
	Residuals	118	3.066	0.026		0.768	
	Total	133	3.990			1.000	

Table S10. Full statistical results for the experimental acute heat stress assay. R^2c indicates the conditional R^2 (e.g., assessment of model fit). Bolding indicates significant p values.

Response variable	Fixed effects	R^2c	Random effect variance	Chisq	Degrees of freedom	p value (Pr > Chisq)
Photochemical yield (Fv/Fm)	(Intercept)	0.83	0.07	1030.2318	1	**< 2.2e-16**
	Treatment			348.3408	3	**< 2.2e-16**
	Species			2.8518	1	0.09127
	Phenotype			0.1034	1	0.74779
	Treatment:Species			35.3168	3	**1.04E-07**
	Treatment:Phenotype			9.1089	3	**0.02788**
	Species:Phenotype			0.2096	1	0.64706
	Treatment:Species:Phenotype			4.4031	3	0.2211
Color score	(Intercept)	0.83	0.17	195.0162	1	**< 2.2e-16**
	Treatment			134.0736	3	**< 2.2e-16**
	Species			7.4448	1	**0.006362**
	Phenotype			6.7526	1	**0.009361**
	Treatment:Species			5.4485	3	0.141749
	Treatment:Phenotype			3.5958	3	0.308551
	Species:Phenotype			4.0853	1	**0.043257**
	Treatment:Species:Phenotype			1.053	3	0.788433

Table S11. Endosymbiont community composition of *Montipora capitata* colonies sampled for this study. Symbiont percentages reflect quantitative PCR results from colony samples collected July 9, 2019 (32).

Colony ID	Bleaching phenotype	*Durusdinium glynnii* (%)	*Cladocopium* 'C31' (%)
3	Susceptible	0	100
4	Resistant	83	17
11	Susceptible	41	59
12	Resistant	98	2
19	Susceptible	0	100
20	Resistant	98	2
201	Susceptible	0	100
202	Resistant	92	8
203	Susceptible	0	100
204	Resistant	96	4
209	Susceptible	0	100
210	Resistant	64	36
211	Susceptible	0	100
212	Resistant	98	2
213	Susceptible	1	99
214	Resistant	98	2
219	Susceptible	0	100
220	Resistant	98	2
221	Susceptible	0	100
222	Resistant	97	3

Table S12. Full information on the statistical models used, including fixed and random effects, statistical tests, estimates of parameters, strength of evidence, and sample sizes (see Tables S3–S4, S7 for sample sizes by fixed effect). [#]Response was evaluated separately for each species.

	Model	Response variable(s)	Fixed effects	Random effects	Sample size (n)	Statistical test	Strength of evidence
In situ bleaching severity	Linear model	Colony-level bleaching severity	Phenotype*Species*Season*Time	N/A	7–10	ANOVA	p value
In situ partial mortality	Linear mixed effects model	Colony-level partial mortality	Phenotype*Species*Time	Colony	9–10	ANOVA	p value
In situ host physiology	Linear mixed effects model	Tissue biomass (ash-free dry weight)	Phenotype*Species*Time	Colony	4–10	ANOVA	p value
	Linear mixed effects model	Protein concentration	Phenotype*Species*Time	Colony	4–10	ANOVA	p value
	Linear mixed effects model	Lipid concentration	Phenotype*Species*Time	Colony	4–10	ANOVA	p value
	Linear mixed effects model	Total antioxidant capacity (TAC)	Phenotype*Species*Time	Colony	4–10	ANOVA	p value
	Linear mixed effects model	Melanin content	Phenotype*Species*Time	Colony	4–10	ANOVA	p value
	Linear mixed effects model	Prophenoloxidase (PPO) activity	Phenotype*Species*Time	Colony	4–10	ANOVA	p value
	Linear mixed effects model	Calcium carbonate ($CaCO_3$) density	Phenotype*Species*Time	Colony	4–10	ANOVA	p value
In situ symbiont physiology	Linear mixed effects model	Symbiont density	Phenotype*Species*Time	Colony	4–10	ANOVA	p value
	Linear mixed effects model	Chlorophyll-*a* concentration	Phenotype*Species*Time	Colony	4–10	ANOVA	p value

Multivariate in situ health metric[#]	Principal components analysis (PCA)	Tissue biomass, protein concentrations, total antioxidant capacity, $CaCO_3$ density, symbiont density, chlorophyll-*a* concentration	Phenotype*Time	N/A	4–10	permutational ANOVA (PERMANOVA)	p value
Experimental physiology	Linear mixed effects model	Photosynthetic yield (Fv/Fm)	Treatment*Phenotype* Species	Colony	10	ANOVA	p value
	Linear mixed effects model	Color score	Treatment*Phenotype* Species	Colony	10	ANOVA	p value
Experimental bleaching threshold[#]	Three-parameter log-logistic dose-response curve (LL.3)	Photosynthetic yield (Fv/Fm)	Temperature*Phenotype	N/A	10	ANOVA	p value
	Three-parameter log-logistic dose-response curve (LL.3)	Color score	Temperature*Phenotype	N/A	10	ANOVA	p value

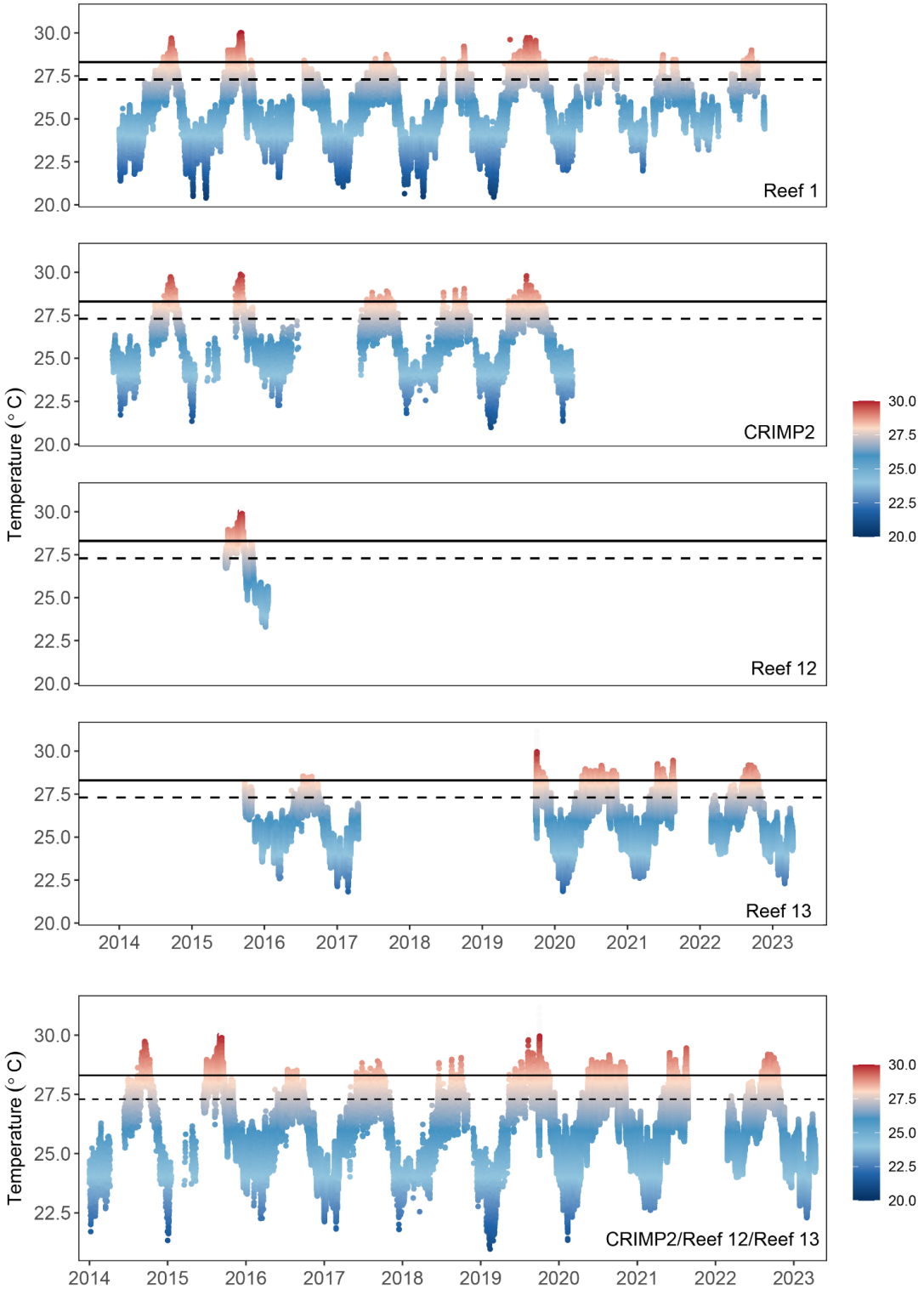

Figure S1. Temperature data from different sites across Kāneʻohe Bay. *In situ* temperatures were recorded from January 2014 – April 2023 at a depth of 0.7–2.7 m in Kāneʻohe Bay. Points indicate hourly measurements. Dashed horizontal line indicates the Kāneʻohe Bay's climatological maximum monthly mean (MMM; 27.3°C) and solid horizontal line indicates the local coral bleaching threshold (MMM+1°C; 28.3°C).

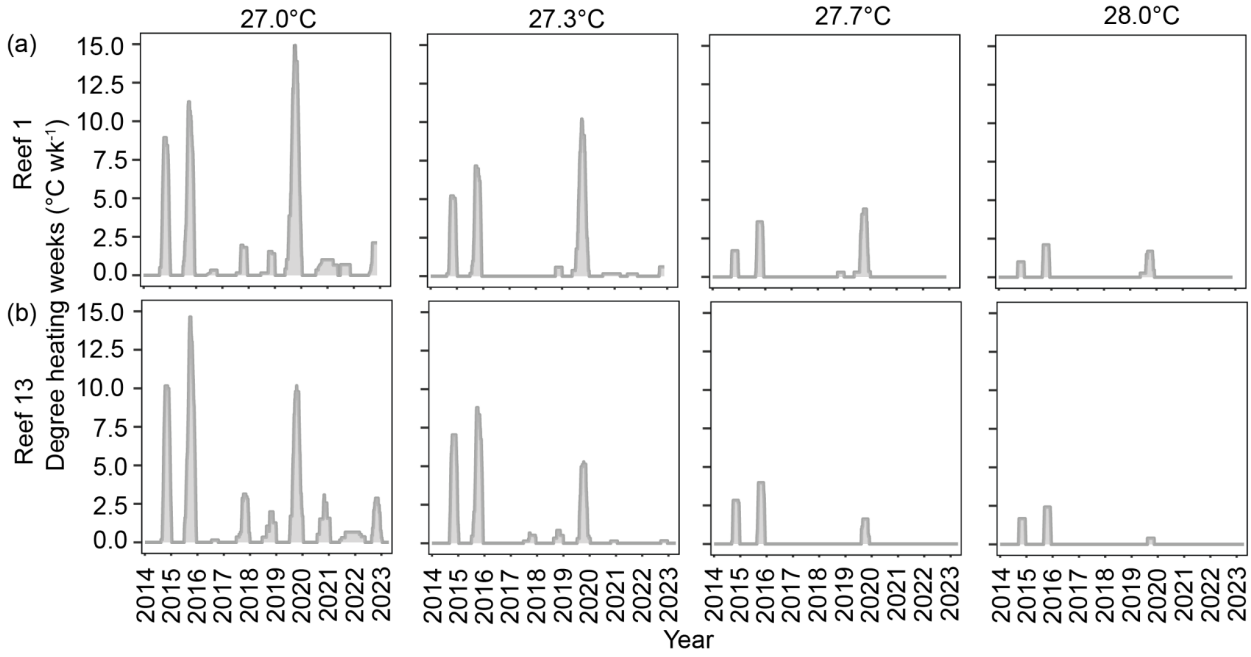

Figure S2. Comparison of degree heating weeks across Kāneʻohe Bay. (a) Degree heating week profiles at at Patch Reef 1 (Moku o Loʻe) calculated using a maximum monthly mean (MMM) of 27.0°C (current regional MMM used by NOAA for the Main Hawaiian Islands) and a range of MMM used for Kāneʻohe Bay: 27.0°C, climatic MMM from 1960s (3); 27.3°C, climatic MMM from 1990s; 27.7°C, used by (4, 5), and 28.0°C, used by (5–7, 33). (b) Degree heating week profiles calculated using a MMM of 27.0°C, 27.3°C, 27.7°C, and 28.0°C at Patch Reef 13.

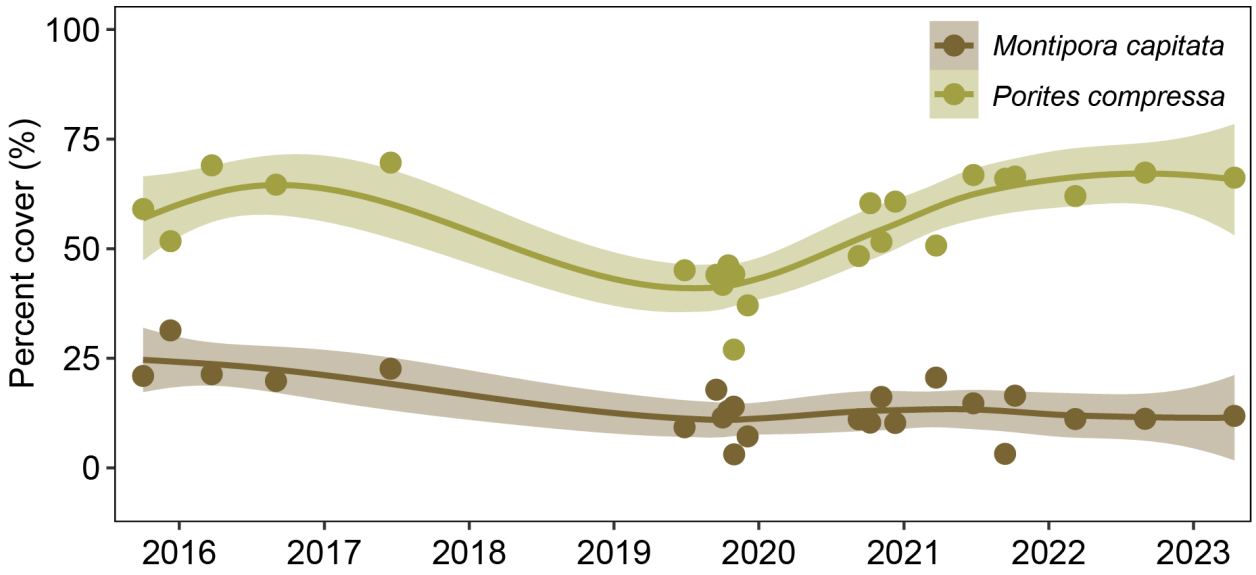

Figure S3. Hard coral cover of species of interest (*Montipora capitata* and *Porites compressa*) at Patch Reef 13 from September 2015–April 2023. Points represent mean percent cover from benthic surveys (n = 2–4), and lines and ribbons represent smoothed conditional means ± 95% CI.

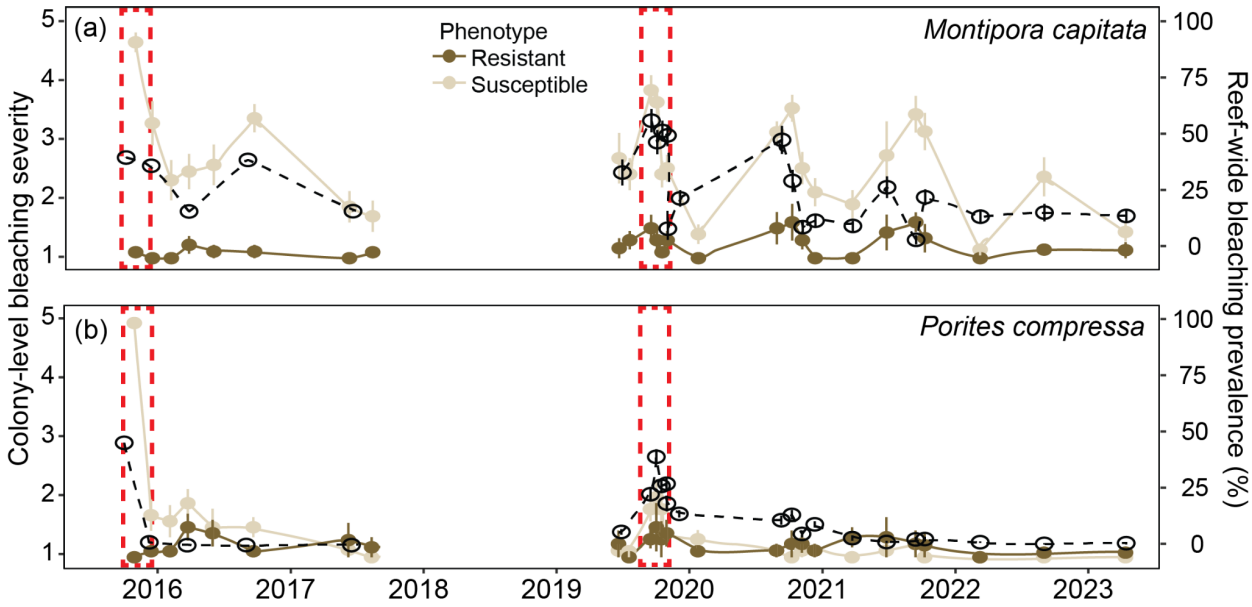

Figure S4. Bleaching response of bleaching-resistant and bleaching-susceptible corals versus reef-wide bleaching prevalence for (a) *M. capitata* (mean ± SE; n = 9–10) and (b) *P. compressa* (mean ± SE; n = 7–10) from September 2015 – April 2023. Colony-level bleaching severity was visually determined for each colony following the methodology of (35), where (1) represents 0% bleached and (5) >80% bleached. Open circles and dashed lines represent mean ± SE of reef-wide bleaching prevalence determined from benthic surveys (n = 2–4 transects per time point) for species of interest. Dashed red rectangles indicate the 2015 and 2019 marine heatwaves.

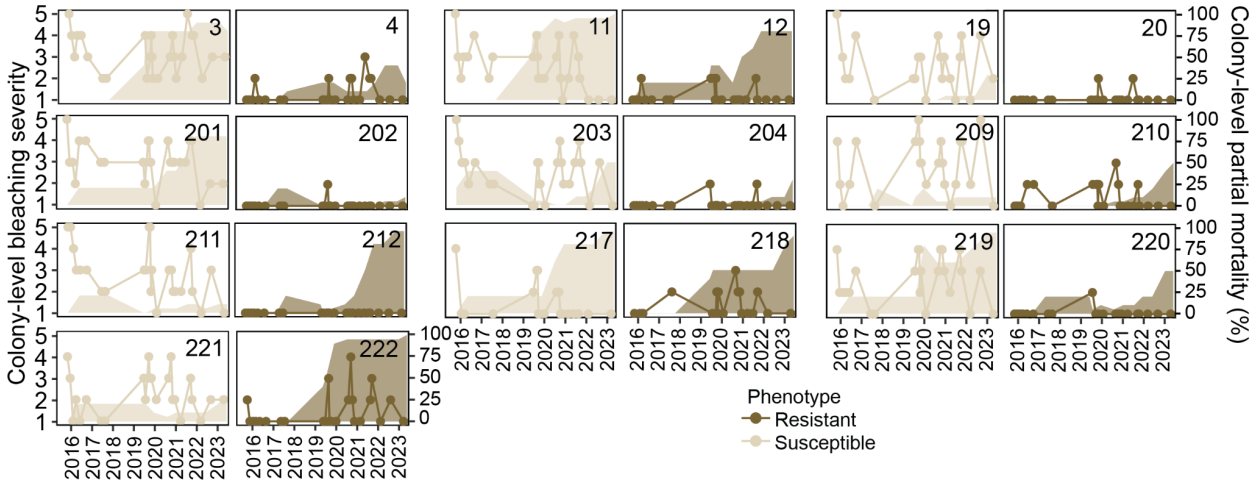

Figure S5. Colony-level bleaching severity and cumulative partial mortality of individual colonies of *Montipora capitata* from September 2015 – April 2023. Colony-level bleaching severity was visually determined for each colony following the methodology of (6), where (1) represents 0% bleached and (5) >80% bleached. Colony identification number is indicated in the top right; graphs for each pair of bleaching-susceptible (odd number) and bleaching-resistant (even number) colonies are consecutively numbered and displayed side by side.

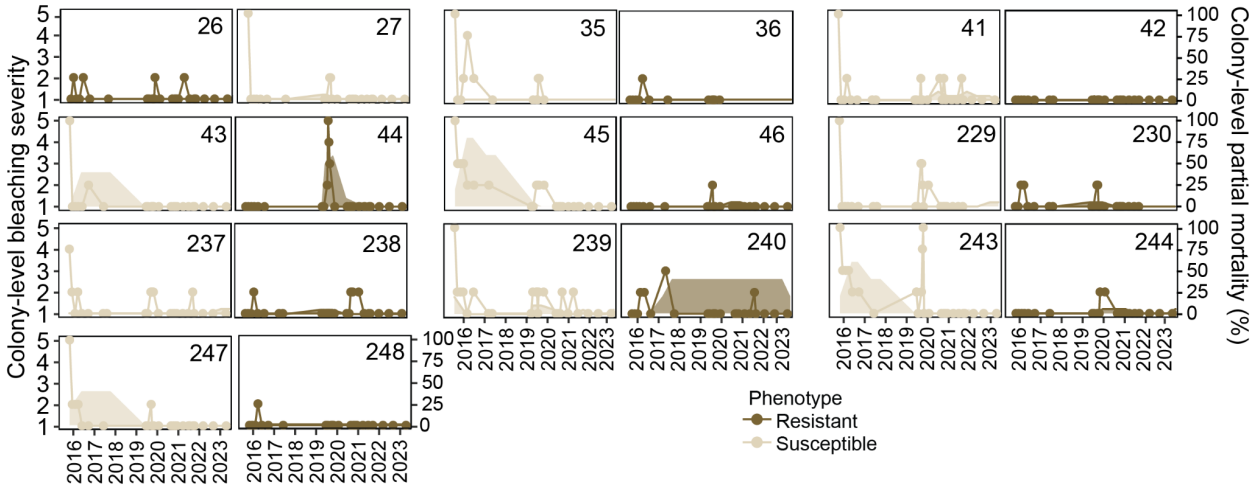

Figure S6. Colony-level bleaching severity and cumulative partial mortality of individual colonies of *Porites compressa* from September 2015 – April 2023. Colony-level bleaching severity was visually determined for each colony following the methodology of (6), where (1) represents 0% bleached and (5) >80% bleached. Colony identification number is indicated in the top right; graphs for each pair of bleaching-susceptible (odd number) and bleaching-resistant (even number) colonies are consecutively numbered and displayed side by side.

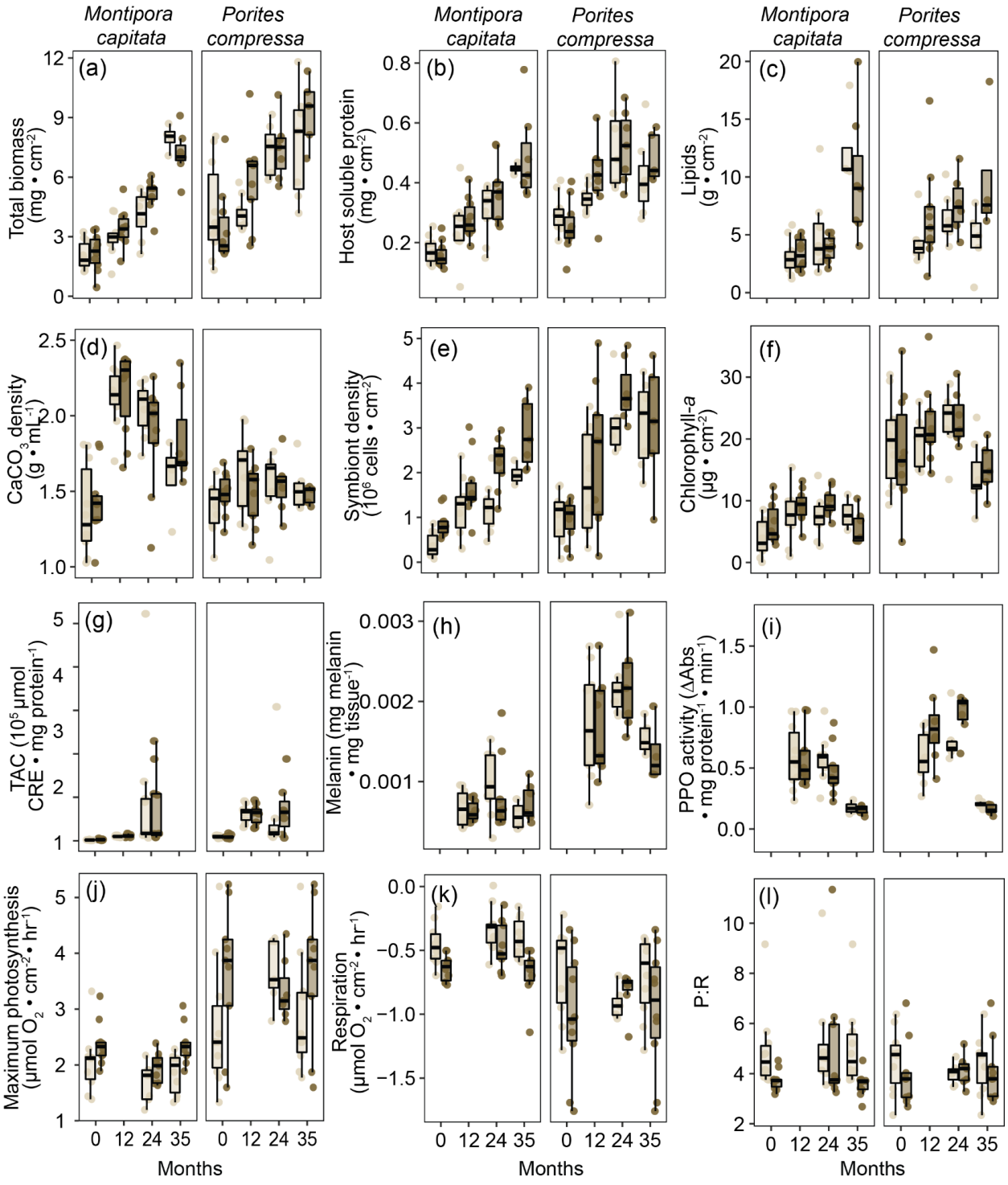

Figure S7. Physiological traits of bleaching-resistant and bleaching-susceptible corals during peak annual temperatures in the years following the 2019 heatwave. Months indicate time post-heat stress, where '0' represents during the 2019 marine heatwave. (a) Host tissue biomass (ash-free dry weight), (b) host soluble protein density, (c) host lipids, (d) calcium carbonate ($CaCO_3$) density, (e) endosymbiont cell density, (f) chlorophyll *a* concentration, (g) host total antioxidant capacity (TAC), (h) host melanin content, (i) host prophenoloxidase (PPO)

activity, (j) maximum photosynthesis, (k) light-enhanced dark respiration, and (l) photosynthesis to respiration ratios (P:R) for bleaching-susceptible and bleaching-resistant *Monitpora capitata* and *Porites compressa*. Boxplots display the minimum, 25th percentile, median, 75th percentile, and maximum, where points indicate individual measures for coral genets (n = 4–10).

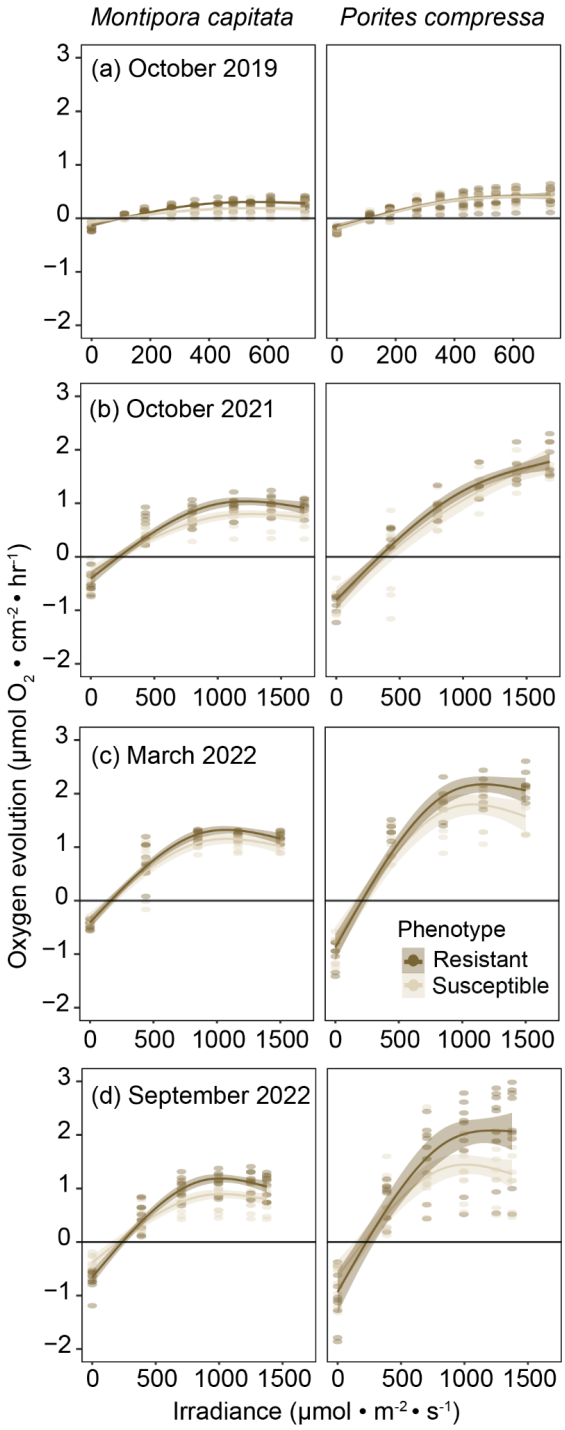

Figure S8. Photosynthesis–irradiance curves of bleaching-susceptible and bleaching-resistant *Monitipora capitata* and *Porites compressa* in (a) October 2019 (during the heatwave; note different x-axis scale), (b) October 2021, (c) March 2022, and (d) September 2022.

Supplemental References

1. K. T. Brown, G. Eyal, S. G. Dove, K. L. Barott, Fine-scale heterogeneity reveals disproportionate thermal stress and coral mortality in thermally variable reef habitats during a marine heatwave. *Coral Reefs*, 1–12 (2022).

2. Rodgers, K. S., P. L. Jokiel, and Western Weather Group, Inc., HIMB Weather Station: Moku o Loe (Coconut Island), Oahu, Hawaii. [1992-2002] Distributed by the Pacific Islands Ocean Observing System (PacIOOS) (2005) (2023).

3. P. L. Jokiel, S. L. Coles, Effects of temperature on the mortality and growth of Hawaiian reef corals. *Mar. Biol.* **43**, 201–208 (1977).

4. C. B. Wall, *et al.*, Shifting baselines: Physiological legacies contribute to the response of reef corals to frequent heatwaves. *Funct. Ecol.* **35**, 1366–1378 (2021).

5. C. P. Jury, R. J. Toonen, Adaptive responses and local stressor mitigation drive coral resilience in warmer, more acidic oceans. *Proceedings of the Royal Society B: Biological Sciences* **286**, 20190614 (2019).

6. T. Innis, *et al.*, Marine heatwaves depress metabolic activity and impair cellular acid-base homeostasis in reef-building corals regardless of bleaching susceptibility. *Glob. Chang. Biol.* **27**, 2728–2743 (2021).

7. S. Matsuda, *et al.*, Coral bleaching susceptibility is predictive of subsequent mortality within but not between coral species. *Frontiers in Ecology and Evolution* **8**, 1–14 (2020).

8. C. Drury, *et al.*, Intrapopulation adaptive variance supports thermal tolerance in a reef-building coral. *Commun Biol* **5**, 486 (2022).

9. C. Caruso, *et al.*, Genetic patterns in Montipora capitata across an environmental mosaic in Kāne'ohe Bay, O'ahu, Hawai'i. *Mol. Ecol.* **31**, 5201–5213 (2022).

10. N. S. Locatelli, J. A. Drew, Population structure and clonal prevalence of scleractinian corals (Montipora capitata and Porites compressa) in Kaneohe Bay, Oahu. *bioRxiv*, 2019.12.11.860585 (2019).

11. C. L. Hunter, GENOTYPIC VARIATION AND CLONAL STRUCTURE IN CORAL POPULATIONS WITH DIFFERENT DISTURBANCE HISTORIES. *Evolution* **47**, 1213–1228 (1993).

12. O. Beijbom, *et al.*, Towards Automated Annotation of Benthic Survey Images: Variability of Human Experts and Operational Modes of Automation. *PLoS One* **10**, e0130312 (2015).

13. P. J. Edmunds, P. S. Davies, Post-illumination stimulation of respiration rate in the coral Porites porites. *Coral Reefs* **7**, 7–9 (1988).

14. T. Platt, C. L. Gallegos, W. G. Harrison, Photoinhibition of photosynthesis in natural assemblages of marine phytoplankton (1981) (February 7, 2023).

15. G. Holmes, Estimating three-dimensional surface areas on coral reefs. *J. Exp. Mar. Bio. Ecol.* **365**, 67–73 (2008).

16. J. Stimson, R. A. Kinzie, The temporal pattern and rate of release of zooxanthellae from the reef coral Pocillopora damicornis (Linnaeus) under nitrogen-enrichment and control conditions. *J. Exp. Mar. Bio. Ecol.* **153**, 63–74 (1991).

17. S. W. Jeffrey, G. F. Humphrey, New spectrophotometric equations for determining chlorophylls a, b, c1 and c2 in higher plants, algae and natural phytoplankton. *Biochem. Physiol. Pflanz.* **167**, 191–194 (1975).

18. S. R. Dunn, M. C. Thomas, G. W. Nette, S. G. Dove, A lipidomic approach to understanding free fatty acid lipogenesis derived from dissolved inorganic carbon within cnidarian-dinoflagellate symbiosis. *PLoS One* **7**, e46801 (2012).

19. L. D. Mydlarz, C. V. Palmer, The presence of multiple phenoloxidases in Caribbean reef-building corals. *Comp. Biochem. Physiol. A Mol. Integr. Physiol.* **159**, 372–378 (2011).

20. L. E. Fuess, W. T. Mann, L. R. Jinks, V. Brinkhuis, L. D. Mydlarz, Transcriptional analyses provide new insight into the late-stage immune response of a diseased Caribbean coral. *R Soc Open Sci* **5**, 172062 (2018).

21. E. Tambutté, *et al.*, Morphological plasticity of the coral skeleton under CO 2-driven seawater acidification. *Nat. Commun.* **6**, 1–9 (2015).

22. K. T. Brown, M. A. Mello-Athayde, Environmental memory gained from exposure to extreme pCO2 variability promotes coral cellular acid–base homeostasis. *of the Royal …* (2022).

23. C. R. Voolstra, *et al.*, Standardized short-term acute heat stress assays resolve historical differences in coral thermotolerance across microhabitat reef sites. *Glob. Chang. Biol.* (2020) https:/doi.org/10.1111/gcb.15148.

24. M. R. Marzonie, *et al.*, The effects of marine heatwaves on acute heat tolerance in corals. *Glob. Chang. Biol.* (2022) https:/doi.org/10.1111/gcb.16473.

25. N. R. Evensen, *et al.*, Empirically derived thermal thresholds of four coral species along the Red Sea using a portable and standardized experimental approach. *Coral Reefs* **41**, 239–252 (2022).

26. H. Wickham, *ggplot2: elegant graphics for data analysis* (Springer, 2016).

27. J. Fox, *et al.*, Package “car.” *Vienna: R Foundation for Statistical Computing* (2012).

28. R. Lenth, H. Singmann, J. Love, P. Buerkner, M. Herve, Emmeans: Estimated marginal means, aka least-squares means. *R package version* **1**, 3 (2018).

29. C. Ritz, F. Baty, J. C. Streibig, D. Gerhard, Dose-Response Analysis Using R. *PLoS One* **10**, e0146021 (2015).

30. J. Oksanen, *et al.*, Package “vegan.” *Community ecology package, version* **2**, 1–295 (2013).

31. P. M. Arbizu, pairwiseAdonis: Pairwise multilevel comparison using adonis (2020) (2021).

32. J. Dilworth, C. Caruso, V. A. Kahkejian, A. C. Baker, C. Drury, Host genotype and stable differences in algal symbiont communities explain patterns of thermal stress response of

Montipora capitata following thermal pre-exposure and across multiple bleaching events. *Coral Reefs* **40**, 151–163 (2021).

33. K. D. Bahr, P. L. Jokiel, K. S. Rodgers, The 2014 coral bleaching and freshwater flood events in Kāneʻohe Bay, Hawaiʻi. *PeerJ* **3**, e1136 (2015).